Comparison Between Typical Pavement Structure In Accordance With Polish Design Guide and Innovation Pavement Structure With Use of Veroad Software

Sybilski D.
Professor, Deputy Director – Road and Bridge Research Institute, Warsaw, Poland

Mularzuk R.
Leader of Asphalt Pavement Laboratory – Road and Bridge Research Institute, Warsaw, Poland

Bankowski W.
Assistant – Road and Bridge Research Institute, Warsaw, Poland

SYNOPSIS

The purpose of work was to compare two flexible asphalt pavement structures: typical in accordance with Polish Catalogue of Typical Flexible and Semi-Rigid Pavements consisted in standard asphalt mixes with conventional binders and innovative of varying layers' thickness with high modulus mixes with polymer modified binders. Asphalt mixtures were subjected to the wide range of laboratory tests: complex modulus test, fatigue test, creep test, rutting test, direct tension-compression test and triaxial creep test. VEROAD software based on viscoelastic models was used for analysis of strains and stresses in the pavements with use of data from laboratory tests. Two basic studies of structures were performed: fatigue life analysis with use of different fatigue criteria and analysis of permanent deformation. The analysis showed advantages of innovative structures and materials, i.e. longer durability and possibility of reduction of pavement thickness. VEROAD software allows for comprehensive and reliable complex assessment of pavement serviceability and for better understanding and prediction of pavement performance.

Comparison Between Typical Pavement Structure In Accordance With Polish Design Guide And Innovation Pavement Structure With Use Of Veroad Software

INTRODUCTION

Purpose of the work was to compare two asphalt pavement structures: typical in accordance with Polish Catalogue of Typical Flexible and Semi-Rigid Pavements (KTKNPP) [Sybilski et al. (1997)] consisted in standard asphalt mixes with conventional binders and innovative with varying layers' thickness, with high modulus mixtures and polymer modified binders. The mixtures were subjected to the laboratory tests: complex modulus test, fatigue test, creep test, rutting test, direct tension-compression test and triaxial creep test. Tests results were used in VEROAD software based on viscoelastic models. Two basic studies of structures were performed: fatigue life analysis with use of different fatigue criteria and evaluation of permanent deformation. The analysis showed advantages of use of innovative structures and materials, i.e. longer durability and possibility of reduction of pavement thickness. Application of VEROAD software allows for comprehensive and reliable complex assessment of pavement serviceability and for better understanding and prediction of pavement performance.

MATERIALS

Binders

Binders used in this study and their basic properties are listed in table 1.

Table 1: Basic properties of the binders

Binder	Type	Pen 25 °C 0,1mm	$T_{R\&B}$ °C	T_{Fraass} °C	PI (Pen/$T_{R\&B}$)
D50P	pure bitumen	51	55.0	-17	0.10
OL30B	polymer-bitumen (SBS)	41	63.5	-15	1.30
OL80C	polymer-bitumen (SBS)	51	76.0	-17	3.81

Aggregates

The following mineral aggregates were used: limestone filer; crushed granite sand 0/2 mm; basalt 2/5 mm; basalt 5/8 mm; basalt 8/11 mm; granite 11/16 mm; granite 16/25 mm.

Asphalt Mixtures

Five different mixtures were designed and tested:
BA25 D50P - asphalt concrete according to Polish Standard PN-S-96025:2000 for base courses in pavements subjected to heavy traffic category KR3-KR6 with D50P bitumen,
BA20 D50P - asphalt concrete according to Polish Standard PN-S-96025:2000 for binder courses in pavements subjected to heavy traffic category KR3-KR6 with D50P bitumen,
BA16 D50P - asphalt concrete according to Polish Standard PN-S-96025:2000 for wearing courses in pavements subjected to heavy traffic category KR3-KR6 with D50P bitumen,
SMA8 OL80C – stone mastic asphalt SMA according to Polish Standard PN-S-96025:2000 for wearing courses in pavements subjected to heavy traffic category KR3-KR6 with OL80C,
BAWMS20 OL30B – high modulus asphalt concrete according to [Sybilski et al. (2002)] for base course and wearing course with OL30B.
Basic properties of mixes are shown in table 2.

Table 2: List of asphalt mixtures

Symbol	Layer	Grading, mm	Binder content, %m/m	Air voids content, %v/v	Marshall stability, kN	Marshall flow, mm
BA25 D50P	base course	0/25	4.0	5.9	12.2	3.0
BA20 D50P	binder course	0/20	4.2	5.6	11.5	2.6
BA16 D50P	wearing course	0/16	4.9	2.9	11.3	2.8
SMA8 OL80C	wearing course	0/8	6.4	2.9	8.8	4.0
BAWMS20 OL30B	base course	0/20	4.2	4.8	12.5	2.6
BAWMS20 OL30B	binder course	0/20	4.2	4.8	12.5	2.6

PAVEMENT STRUCTURES

In this work two types of structures were analysed:
typical "T" – structure according to Catalogue [Sybilski et al. (1997)]. This structure consisted in typical asphalt concrete mixes with pure asphalt D50P (table 3). These mixes are rather coarse with relatively low asphalt content.
innovative "I" – structure consisted in layers shown in table 4. Each layer was made of mixture according to recommendations [Sybilski et al. (2002)]. Wearing course is designed as a thin layer made of SMA8 OL80C. Binder and base course are made of high modulus asphalt concrete BAWMS20 OL30B.

Table 3: Typical pavement structure (T)

Layer	Thickness	Mix
wearing course	5 cm	BA16 D50P
binder course	8 cm	BA20 D50P
base course	18 cm	BA25 D50P
unbound base course	20 cm	crushed aggregate mixture

Table 4: Innovative pavement structure (I)

Layer	Thickness	Mix
wearing course	2 cm	SMA8 OL80C
binder course	6 cm	BAWMS20 OL30B
base course	up to 18 cm	BAWMS20 OL30B
unbound base course	20 cm	crushed aggregate mixture

TEST METHODS

Fatigue and Complex Modulus

Fatigue tests were performed by means of 4 Point Bending Test according to AASHTO TP8-94 (1994) with use of MTS universal material testing machine. Four point bending test consists in cycling bending of rectangular beam at constant amplitude deflection (tensile strain). Test conditions were as follows: temperature 10 °C; frequency 10 Hz; sinusoidal loading; constant strain mode.
The temperature of 10 °C is the equivalent temperature for Poland for fatigue life analysis, as it was proven in the study performed according to the procedure developed in SHRP, Cominsky (1997), and according to French method (1997).
Fatigue causes microcracking of sample and decrease in stiffness modulus of the beam. Fatigue life (N_f) is defined as a number of cycles, when stiffness modulus is reduced to 50 % of the initial value.
Typical fatigue law is described as follows:

$$N_f = A \cdot \varepsilon^b \quad \text{Equation 1}$$

where:

N_f – fatigue life,
ε – strain amplitude,
A, b – material factors evaluated in linear regression.

This equation is a fatigue law of asphalt mixture at a given temperature. The curve in logarithmic scales representing the fatigue life versus the amplitude of the applied loading is the material's Wöhler's curve.

The 4 Point Bending Test method and the same equipment were used to perform complex modulus test. Test conditions were as follows: temperature 0, 10, 20, 30 °C; frequency 0.1, 1, 5, 10, 20, 30 Hz; sinusoidal loading; constant strain of 30 μm/m.

Complex modulus is described by a complex number that is characterized by the following equation:

$$E^* = E' + iE'' \qquad \text{Equation 2}$$

where:

E' – real part (elastic),
E'' – imaginary part (viscous).

Both parts are tied together with value of phase angle:

$$tg\varphi = \frac{E''}{E'} \qquad \text{Equation 3}$$

where:

φ - phase angle, °.

Stiffness modulus is defined as the absolute value of complex modulus:

$$E = |E^*| \qquad \text{Equation 4}$$

Direct Tension and Compression Tests

Tensile and compression strength were tested according to the procedure by IBDiM that is based on VEROAD procedure, Hopman et al. (1997). Tests were conducted on cylindrical Marshall specimens. In compression, test loading was applied axially directly on the sample. Samples for tensile tests were glued to two plates with use of special equipment that assured axial loading and parallelism.

Specimens were loaded with displacement speed of 0,425 mm/s. Maximum force at break at given test temperature is the test result. Tensile or compression strength is given by the following law:

$$\sigma_r = \frac{F_r}{P} \qquad \text{Equation 5}$$

where:

σ_r – tensile or compression strength, MPa,
F_r – maximum force at break, N,
P – cross-section before a test, mm^2.

Tensile and compression strength were used to draw failure line on Mohr-Coulomb chart.
The failure line is described by cohesion C and angle of internal friction $\tilde{\phi}$.

Repeated Triaxial Creep Test With Static Confining Pressure

Repeated triaxial creep test with static confining pressure (triaxial test) was performed according to the procedure of IBDiM based on prEN 12697−25, 2003 in agreement with VEROAD recommendations, and the study on triaxial compression test, Molenaar and Molenaar, 200.Tests were conducted on cylindrical, properly compacted and prepared Marshall specimens. Test temperature was 40 °C. Confining pressure of 0,05 MPa was applied with use of modifying Hveem device. Vertical loading was applied by MTS testing machine. Minimum vertical stress σ_{1min} was equal to confining pressure σ_3 and maximum vertical stress σ_1 was 0,5 MPa. Duration of minimum vertical stress σ_{1min} was 0,8 s and duration of and maximum vertical stress σ_1 was 0,2 s. Strain measurement were taken at the beginning of each maximum stress.

Creep curve is derived in logarithmic scales as a strain in function of time. In a curtain range of load cycles (usually between 100 and 7200) this creep curve is very closed to the line with slope a. Inverse value of tangent of this slope is considered as viscosity η of mix at given temperature, loads and dimensions of sample. It is characterized is the following equation:

$$\sigma = \eta \cdot \frac{d\varepsilon}{dt} = \eta \cdot \frac{d\varepsilon}{dN} \cdot \frac{dN}{dt} = \eta \cdot \alpha \cdot \beta \qquad \text{Equation 6}$$

where:

σ – stress deviator, $\sigma = \sigma_1 - \sigma_3$
σ_1 – vertical principal stress,

σ_3 – confining principal stress,
η – viscosity,
α – tangent of slope of straight line,
β – constant depended on function between cycle time and duration of maximum stress.

Therefore viscosity in our tests was characterized by equation:

$$\eta = \frac{0{,}09}{\alpha}$$ Equation 7

VISCOELASTIC MODELS

General

Model of pavement behaviour subjected to loading imposed by moving wheels is needed to calculate stresses and strains in the structure. Conventional models used in pavement design assume static loading (wheel is immobile) and materials are working according to the linear elastic law. More advanced models assume visco-elastic behaviour of materials. They consist in various combinations of springs and dashpots. VEROAD software uses Burgers model and Huet-Sayegh model.

Burgers Model

Diagram of Burgers model is shown on figure 1. Viscoelastic behaviour of bituminous materials is characterized by linear elastic bulk modulus K and linear viscoelastic shear modulus G*. It is assumed that volume of material is changed under applied load and it is reversible. This is simulated by spring E. Spring E_1 and dashpot η_1 are responsible for spring deformations and dashpot η causes viscous deformations. That model is used in calculation of stresses and strains in pavement structure subjected to moving loads at given conditions. This model is also used for prediction of permanent deformation, but then it is reduced to one dashpot η. Parameters of Burgers model E, E_1, η, η_1 are derived from analysis of results from complex modulus test with use of DEBUROAD software. Complex modulus E* is described by Burgers model:

$$E^*(i\omega) = \frac{E}{1+(i\omega\frac{\eta}{E})^{-1}} + \frac{E_1}{1+(i\omega\frac{\eta_1}{E_1})^{-1}}$$ Equation 8

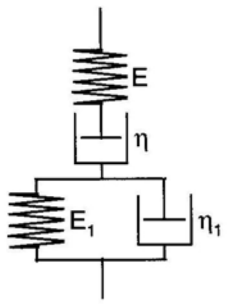

Figure 1: Burgers model

Huet-Sayegh Model

Huet-Sayegh model consist in two parallel branches of which one consists of two biparabolic dashpots k and h and a spring E_∞ - E_0 in series and the other one consists in single spring E_0. E_∞ represents the purely elastic modulus, and E_0 means long-term solid behaviour of asphalt, Hopman et al. (2001) (figure 2). Complex modulus E* is described by Huet-Sayegh model with following equations:

$$E^*(i\omega) = E_0 + \frac{E_{\infty-0}}{1+\delta(i\omega\tau)^{-k} + (i\omega i\omega^{-h}}$$ Equation 9

$$ln(\tau) = a + bT + cT^2$$ Equation 10

Parameters of Huet-Sayegh model E_∞, E_0, k, h, δ are derived from analysis of results from complex modulus test with use of Excel calculation sheet HUSAROAD.

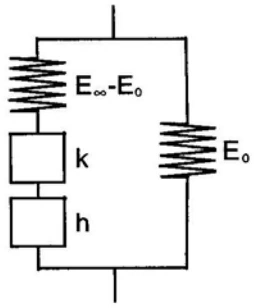

Figure 2: Huet-Sayegh model

TEST RESULTS

Fatigue

Fatigue tests were performed on mixes for base course: BA25 D50P and BAWS20 OL30B. Fatigue lines and laws are presented on figure 3.

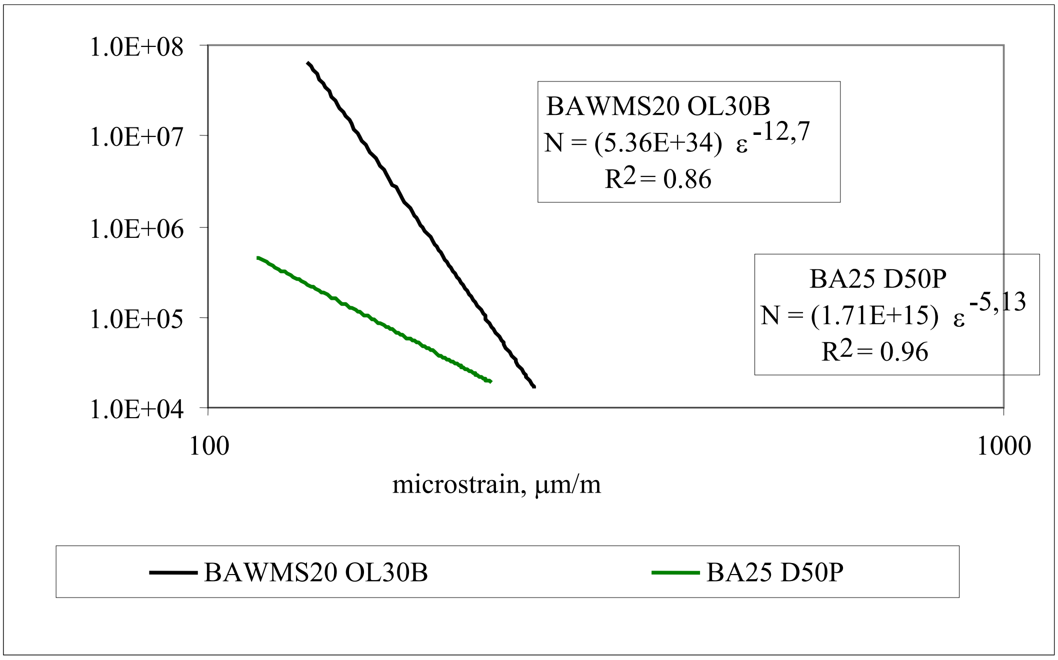

Figure 3: Fatigue lines and laws

Complex Modulus

Results of complex modulus tests were used to calculate the parameters of Burgers and Huet-Sayegh model (table 5 and 6).

Table 5: Parameters of Burgers model

Temperature	Weight	E_1	E_2	η_1	η_2
°C	-	MPa	MPa	MPa.s	MPa.s
BA16 D50P					
40	10	352	40	1996	515
30	10	3395	1350	912	90
20	10	6687	3939	2473	230
10	10	12337	13956	8633	735
0	10	20032	37580	23475	1486
BA20 D50P					

40	10	406	45	2136	609
30	10	3333	1390	1067	90
20	10	7584	4929	3128	275
10	10	14000	14582	9847	637
0	10	18945	46437	27845	2203
BA25 D50P					
40	10	1573	1223	118	59
30	10	324	152	3506	3693
20	10	8598	10613	927	357
10	10	14853	29806	2547	705
0	10	21296	81936	6653	2251
SMA8 OL80C					
40	10	158	15	879	187
30	10	1659	593	576	38
20	10	5541	2306	1559	153
10	10	11295	8659	5271	458
0	10	19564	32872	19217	1401
BAWMS20 OL30B					
40	10	461	50	2325	646
30	10	3748	1552	1274	97
20	10	7913	5128	3404	295
10	10	14259	18687	11503	1014
0	10	20795	49872	29559	2074

Table 6: Parameters of Huet-Sayegh model

Mixture	E_0, MPa	$E_{\infty-0}$, MPa	k	h	δ	a	b	c
BA16 D50P	130	44 870	0,2000	0,5700	3,3000	0,2475	-0,3437	0,0020
BA20 D50P	170	43 978	0,1918	0,5465	2,8464	0,1058	-0,2980	0,0003
BA25 D50P	81	45 573	0,1791	0,5825	3,3875	1,2235	-0,3758	0,0025
SMA8 OL80C	135	46 016	0,2005	0,5803	2,7093	-0,9583	-0,3245	0,0007
BAWMS20 OL30B	79	33 573	0,2422	0,5338	2,6094	1,6255	-0,3269	0,0009

Direct Tension and Compression

The following parameters were assumed in the calculations: temperatures of 10 ºC and 40 ºC; Poisson's ratio for bitumen layers at 10 ºC was 0,3 and for 40 ºC was 0,35; Poisson's ratio for sub-base and sub-soil was 0,3; stiffness modulus for sub-base was 400 MPa; stiffness modulus for sub-soil was 100 MPa; wheel load on pavement was 50 kN; contact pressure 0,7 MPa (radius of the wheel to pavement contact area was 0,15 m); there was no horizontal force; vehicle speeds were 5 km/h and 60 km/h (1,4 m/s and 16,7 m/s); pavement courses were fully joined together;

Assuming the absence of horizontal force in the Y-axis direction, strain and stress are symmetric in the X-axis direction – direction of the vehicle movement.

Results of direct tension and compression tests were the basis for calculating parameters of the failure line, shown in the table 7.

Table 7: Cohesion and angle of internal friction at 40 °C

No.	Asphalt	Angle of internal friction ϕ, °	Cohesion C, MPa
1	BA16 D50P	54,1	0,8
2	BA20 D50P	57,8	0,8
3	BA25 D50P	60,8	0,7
4	SMA8 OL80C	55,1	0,5
5	BAWMS20 OL30B	57,1	0,8

Repeated Triaxial Creep Test With Static Confining Pressure

The viscosity η of asphalt mixes were calculated on the basis of the creep test. Results are shown on the figure 4.

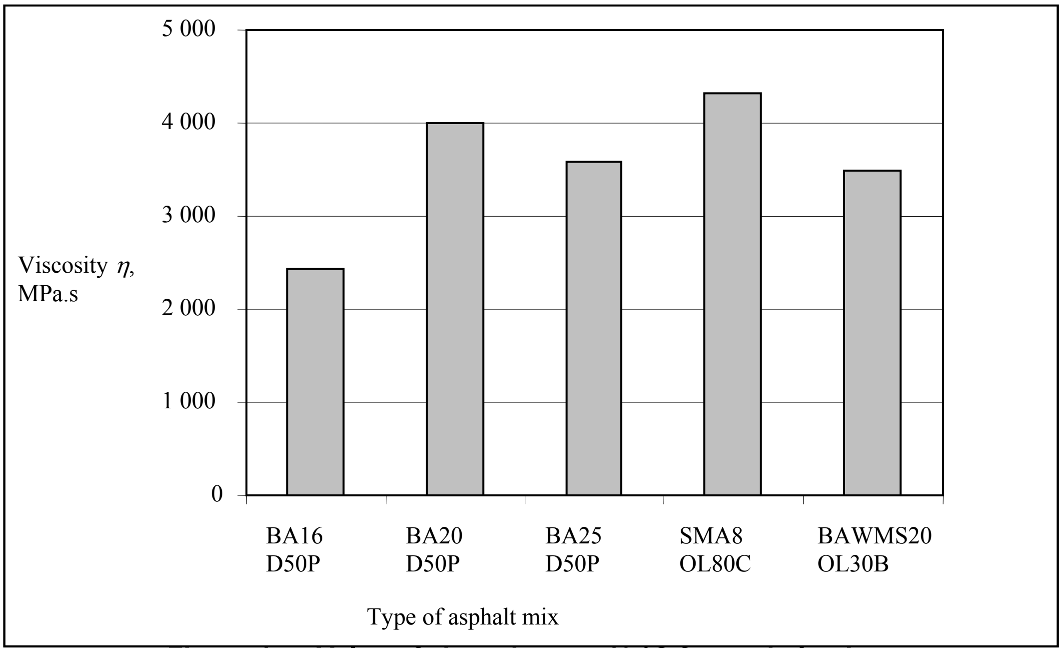

Figure 4: Value of viscosity η at 40 °C for asphalt mixes

ANALYSIS

Fatigue Life of Pavement Structures

Calculations were made for structure „T" and „I". Fatigue life of pavement structures was estimated with use of the following methods:
on the basis of fatigue laws from laboratory fatigue tests,
The Asphalt Institute fatigue law:

$$N_f = 18{,}4 \cdot 10^{4{,}84 \cdot (Vb/(Vv+Vb) - 0{,}69)} \cdot (6{,}167 \cdot 10^{-5} \cdot \varepsilon^{-3{,}291} \cdot E^{-0{,}854}) \qquad \text{Equation 11}$$

where:

E – stiffness modulus, MPa,
Vb – binder content (by volume), %,
Vv – air voids content (by volume), %
ε - strain, m/m.

Parameters *E*, *Vb* and *Vv* were taken from laboratory test results. Strain ε at the bottom of asphalt layers was calculated on the basis of elastic model (BISAR software) and viscoelastic models (Burgers and Huet-Sayegh - VEROAD).

The following assumptions were made for BISAR calculations: Poisson ratio of 0,3 for each layer; axle load of 100 kN; contact pressure of 700 kPa; equivalent temperature of 10 °C.

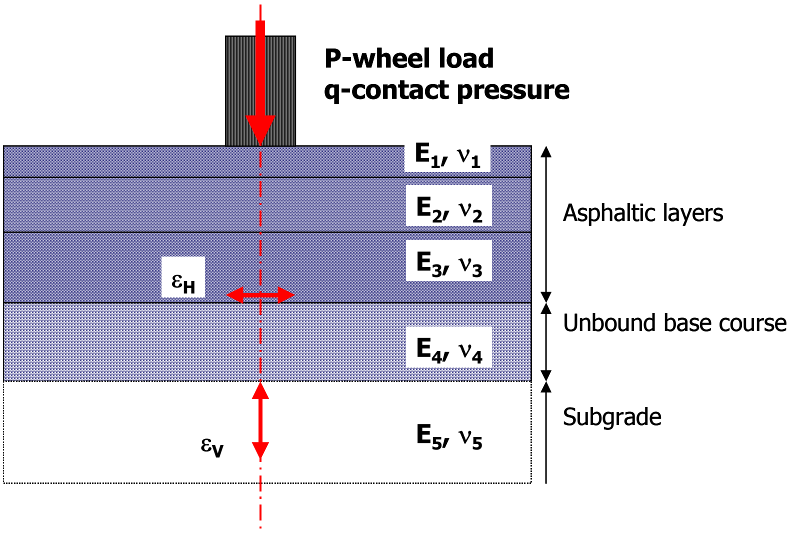

Figure 5: Model of pavement for elastic calculation

The following assumptions were made for VEROAD calculations: Poisson ratio of 0,3 for each layer; axle load of 100 kN; contact pressure of 700 kPa; speed of 60 km/h; equivalent temperature of 10 °C.
Behaviour of asphalt layer in pavement structure subjected to moving loads is viscoelastic, i.e. maximum of tensile strain is delayed with reference to maximum of tensile stress. Elastic models assume that there is no phase delay between these two signals. Moreover, viscoelastic models enable to take into account a speed of wheel that influence behaviour of asphalt mixes. Additionally, VEROAD software enables to calculate the strains at various position of the wheel with reference to the point of calculation. Calculations are performed for a certain number of positions that represent approaching and driving away of a wheel. This is quite important, because in viscoelastic model and in practice maximum of strain appears when a wheel has already passed the calculation point. Results of calculations are listed in table 8.

Table 8: Results of strain and fatigue life calculations

Structure	Elastic model			Burgers model			Huet-Sayegh model		
	ε µm/m	N_{IA} (mln)	N_{IBDM} (mln)	ε µm/m	N_{IA} (mln)	N_{IBDM} (mln)	ε µm/m	N_{IA} (mln)	N_{IBDM} (mln)
„T"	36,7	63,5	161	45,8	30,6	51,6	40,8	44,8	93,4
„I" (18)*	46,8	54,8	429572	53,1	36,1	125073	50,5	42,6	204258
„I" (15)*	56,2	30,0	71848	62,4	21,2	25845	59,4	25,0	41825
„I" (14)*	60,0	24,2	37914	66,1	17,6	14722	63,0	20,6	23538
„I" (13)*	64,0	19,5	20181	70,0	14,6	8408	66,9	16,9	13089
„I" (12)*	68,5	15,6	10396	74,2	12,0	4759	71,1	13,8	7220

* Brackets include thickness of asphalt base course in cm

Tensile strains at a bottom of asphalt layers in elastic analysis are estimated under the centre of wheel and their values are independent of the direction. Viscoelastic analysis shows that maximum of strain appears slightly behind a passing wheel and longitudinal strain ε_{xx} is lower than transversal strain ε_{yy}. Example of tensile strains is shown on figure 6.

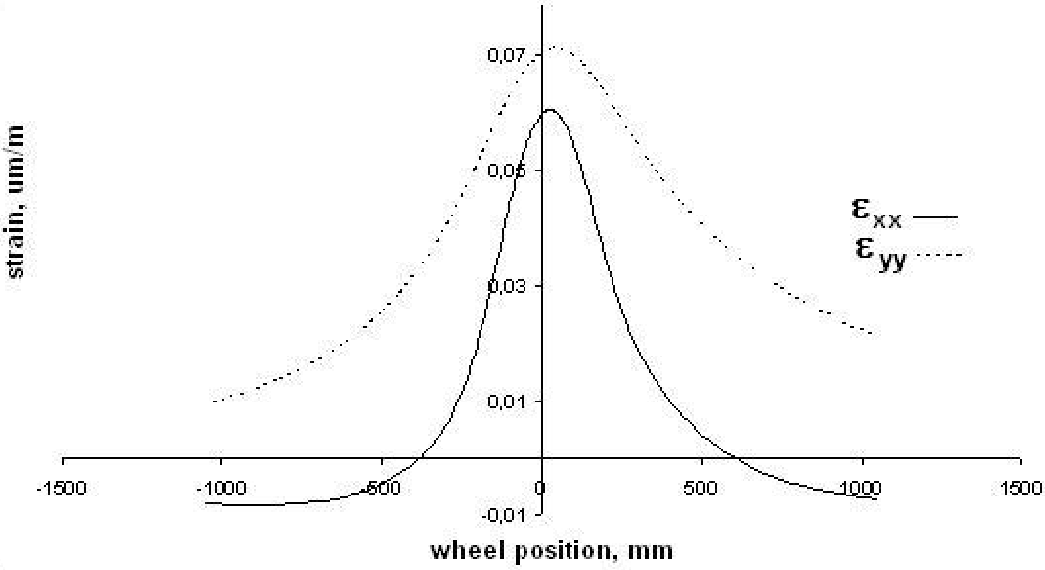

Figure 6: Tensile strains at a bottom of asphalt layers (structure „I" (12), Huet-Sayegh model)

Analysis of all variants leads to the conclusion, that for given structure the lowest calculated tensile strain was always obtained in elastic method, and the highest according to the Burgers model. These differences are between 5 and 15 % and they consequently lead to differences in fatigue life. The typical structure according to [**Errore. Il segnalibro non è definito.**] is characterized by good fatigue life that meets requirements for polish heavy traffic category KR6. The initial innovative structure has thickness of asphalt layer 5 cm lower than typical structure. Fatigue life for "I"(18) structure is very closed to fatigue resistance of typical structure (according to IA). Reduction of 6 cm in thickness of asphalt layers in "I" structure gives fatigue life, which still is appropriate for this traffic category. Calculations with direct use of fatigue laws from IBDiM laboratory show extremely high fatigue life comparing to these according to IA method. This conventional method was worked out on mixes with pure bitumen and it doesn't prove advantages of application of novel materials. On the other hand the shift factor for novel materials should be estimated.

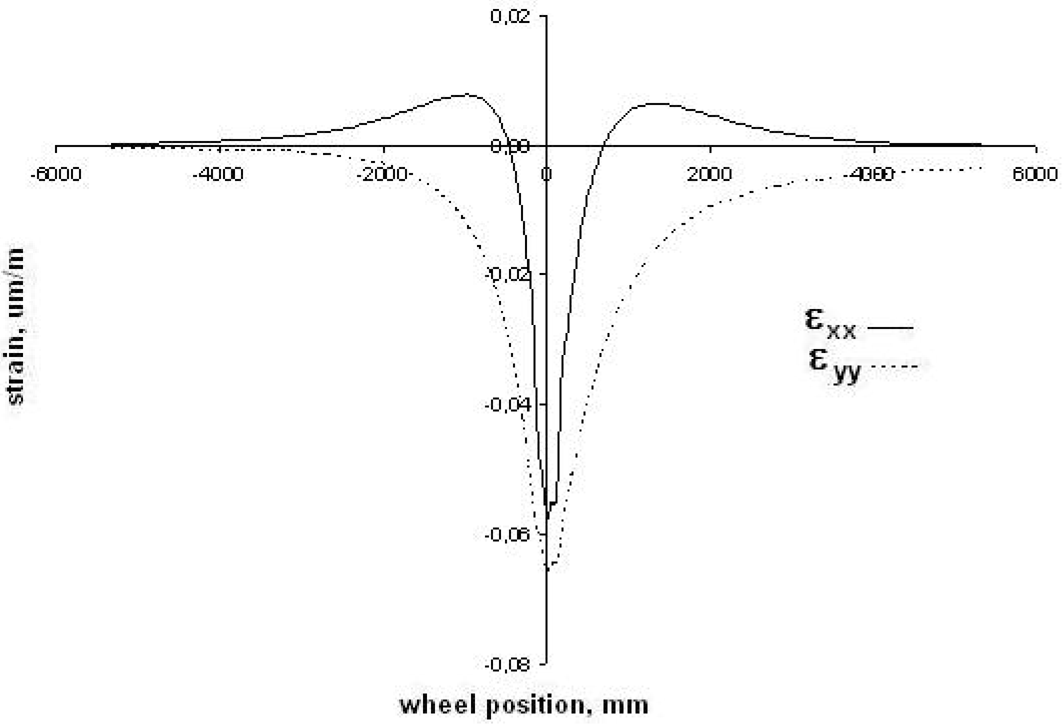

Figure 7: Tensile strains in upper surface of wearing course (structure „I" (12), Huet-Sayegh model)

Our analysis confirmed that tensile strains also appear in wearing course. This phenomenon cannot be detected with conventional analysis with use of linear elastic model. It confirms real observations, that fatigue

cracks may be initiated in the upper part of pavement structure, especially in case of poor bonding between upper asphalt layers and high loads (overloaded trucks, higher contact pressures). Tensile strains in wearing course are illustrated on figure 7.
Maximum tensile strain in the example on figure 7 was about 10 % of maximum strain at the bottom of asphalt layer. This value is rather low, but it could be dangerous for thin layers and it confirms a necessity of using polymer-modified binders for wearing courses.
An influence of speed on tensile strain at the bottom of asphalt layers was analysed. Results are shown in table 9 and figure 8 (structure "I" (12)).

Table 9: Influence of speed

Speed, km/h	Strain, μm/m		Fatigue life (IA), axles (10^6)	
	Burgers model	Huet-Sayegh model	Burgers model	Huet-Sayegh model
80	71,4	68,3	13,6	15,8
60	74,2	71,1	12,0	13,8
45	78,0	74,2	10,2	12,0
30	84,8	79,2	7,7	9,7

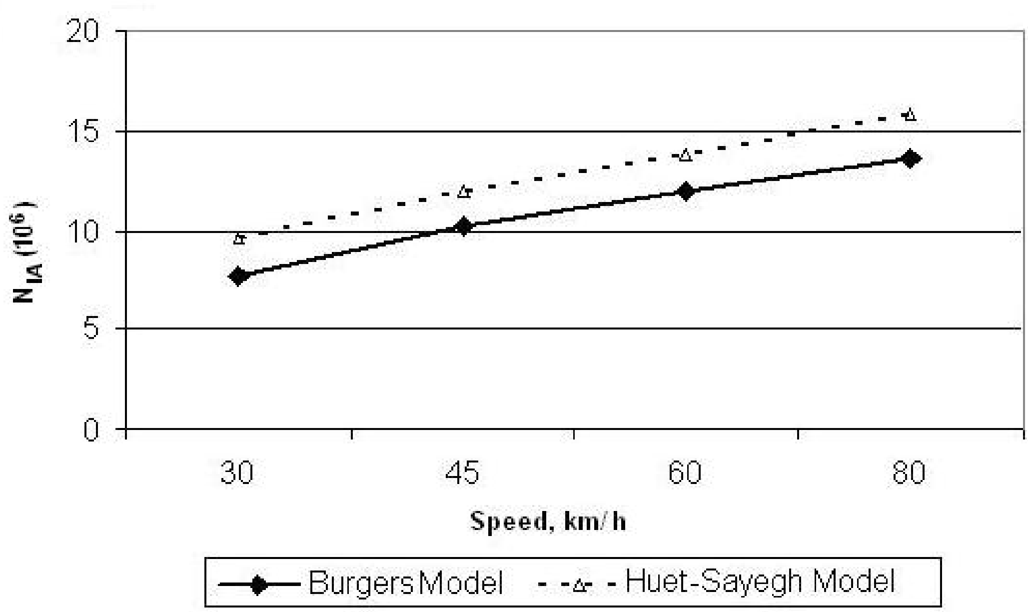

Figure 8: Influence of speed on fatigue life

Table 10 and figure 9 shows thickness needed to carry traffic of at least $14,6*10^6$ axles at various speed of wheel.

Table 10: Influence of speed on fatigue life

Speed, km/h	Thickness of base course, cm		Strain, μm/m		Fatigue life (IA), axles (10^6)	
	Burgers model	Huet-Sayegh model	Burgers model	Huet-Sayegh model	Burgers model	Huet-Sayegh model
80	12,5	11,5	69,3	70,5	14,2	15,0
60	13,0	12,5	70,0	68,9	14,6	15,3
45	14,0	13,0	69,6	69,8	14,8	14,7
30	15,5	14,0	69,9	70,4	14,6	14,3

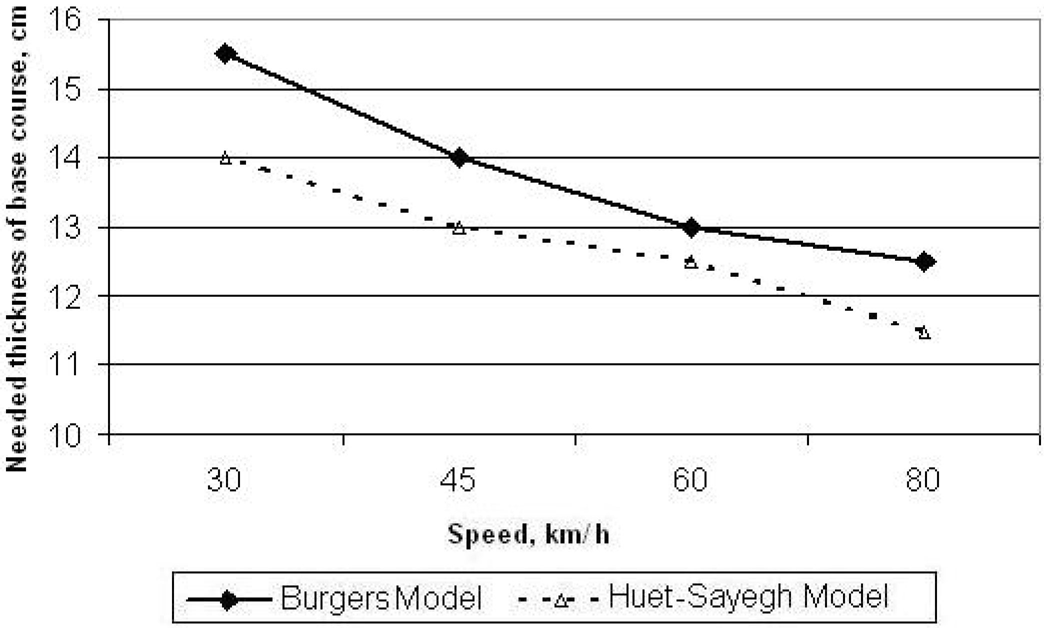

Figure 9: Thickness needed to carry traffic of at least 14,6*10^6 axles at various speed of wheel

Analysis of speed influence shows its quite important impact on fatigue life and thickness of structure. Difference in fatigue life between 30 and 80 km/h is even almost 100 % and difference in thickness of asphalt layers is up to 3 cm. Taking into consideration speed of wheel may be especially important on road sections subjected to low-speed traffic, e.g. on hills.

Permanent deformations

Burgers' Model doesn't take into consideration plastic deformations, so whole analysis acquires to non-plastic phase of the construction work. To find out, if plastic deformations can be omitted during the analysis of construction work, the criteria of Dutch researchers should be applied [**Errore. Il segnalibro non è definito.**] on the basis of Mohr-Coulomb chart analysis. A first criterion is the *R* coefficient according to equations 12 i 13. A second criterion is *F* coefficient according to equation 14.

$$R = \frac{\sigma_1 - \sigma_3}{\sigma_{1,f} - \sigma_3} \quad \text{Equation 12}$$

$$\sigma_{1,f} = \frac{(1+\sin\varphi)\cdot\sigma_3 + 2\cdot C\cdot\cos\varphi}{1-\sin\varphi} \quad \text{Equation 13}$$

$$F = \frac{2\cdot A\cdot C\cdot\cos\varphi}{\sigma_1\cdot(1-\sin\varphi) - \sigma_3\cdot\{[1-(1-2\cdot A)]\cdot\sin\varphi\}} \quad \text{Equation 14}$$

where:

σ_1 - first principal stress in the asphalt construction,
σ_3 - third principal stress in the asphalt construction,
$\sigma_{1,f}$ - first failure stress of the material,
C- cohesion,
φ - angle of internal friction,
A - coefficient of safety, which should equal 1.

The less value *R* coefficient has, the more stable material is and there is less chance of presence of plastic deformations. If *R* coefficient takes values less then 0,3, plastic deformations can be omitted in that case. *F* coefficient defines how many times we can raise the stress before material's failure.

For the limit state of stress analysis the most important are maximum stress values. Computing for stress and strain analysis was made on typical asphalt construction for many measuring points, for Burgers Model, at temperature of 10 °C and vehicle movement speed of 5 km/h. It turned out, that maximum stress and strain were gained directly under the wheel or in closest surrounding of the wheel up to 300 mm. Maximum values of *R* and *F* coefficients are shown in tables 11 and 12.

Table 11: R and F coefficients in asphalt layers; Burgers Model at 40 °C

Depth z, mm	5 km/h						60 km/h					
	"T"		"I" (10)		"I" (16)		"T"		"I" (10)		"I" (16)	
	Coef. *R*	Coef. *F*	Coef. *R*	Coef. *F*	Coef. *R*	Coef. *F*	Coef. *R*	Coef. *F*	Coef. *R*	Coef. *F*	Coef. *R*	Coef. *F*
0	0,02	8,4	0,04	5,4	0,05	5,3	0,05	7,0	0,08	4,6	0,08	4,7
20	0,07	10,0	0,08	10,0	0,08	10,0	0,07	10,0	0,09	6,7	0,08	10,0
50	0,06	10,0	0,08	10,0	0,07	10,0	0,06	10,0	0,09	7,8	0,08	10,0
90	0,05	10,0	0,07	10,0	0,07	10,0	0,06	10,0	0,11	5,2	0,09	7,7
130	0,08	5,5	0,06	9,4	0,07	10,0	0,07	8,1	0,10	3,9	0,09	6,3
190	0,07	6,4	-	-	0,05	10,0	0,07	4,9	-	-	0,08	4,0
250	0,06	4,8	-	-	-	-	0,10	2,4	-	-	-	-

Table 12: R and F coefficients in asphalt layers; Huet-Sayegh Model at 40 °C

Depth z, mm	5 km/h						60 km/h					
	"T"		"I" (10)		"I" (16)		"T"		"I" (10)		"I" (16)	
	Coef. *R*	Coef. *F*	Coef. *R*	Coef. *F*	Coef. *R*	Coef. *F*	Coef. *R*	Coef. *F*	Coef. *R*	Coef. *F*	Coef. *R*	Coef. *F*
0	0,01	9,5	0,05	5,2	0,04	5,4	0,03	8,9	0,07	4,8	0,06	5,0
20	0,08	10,0	0,09	10,0	0,09	10,0	0,08	10,0	0,10	5,9	0,09	10,0
50	0,06	10,0	0,08	10,0	0,07	10,0	0,06	10,0	0,09	9,3	0,08	10,0
90	0,06	10,0	0,07	10,0	0,07	10,0	0,06	10,0	0,10	7,8	0,08	10,0
130	0,07	10,0	0,06	10,0	0,06	10,0	0,08	6,9	0,09	4,8	0,08	8,8
190	0,05	10,0	-	-	0,05	10,0	0,07	6,2	-	-	0,07	5,0
250	0,04	10,0	-	-	-	-	0,06	3,5	-	-	-	-

Three types of constructions were compared: typical – "T", innovative with asphalt layer thickness of 100 mm – "I" (10), and innovative with asphalt layer thickness of 160 mm – "I" (16). On the surface (Depth equals 0) the main stress are closer to failure line in the innovative constructions "I", when the vehicle movement speed was 5 km/h. In the lower part of the construction (130 mm) main stress is closer to the failure line in case of typical construction "T". There is a difference between both of the innovative constructions "I" visible at depth of 0 mm and 130 mm, where worse parameters are in the "I" (16), and at depth of 50 mm worse parameters are in the "I" (10) construction. At speed of 60 km/h there are better parameters on every depth in the typical "T" construction, which is thickest. The worse parameters in this case were gained for thinnest construction – "I" (10).

Comparing the state of stress in particular types of constructions depending on the vehicle movement speed, it is typical that worse conditions are at speed of 60 km/h. The higher speed is, the generated strain is bigger in the construction.

At both speeds in all these constructions the best conditions take place on the surface. There is slightly lowest risk of achieving the plastic deformation. At speeds of 5 km/h in the innovative constructions "I" the worst conditions of the state of stress are achieved at depth of about 20 – 50 mm. In the deeper areas the state of stress is better. The same acquires to the typical construction "T". The speed of 60 km/h causes another stress distribution. Extreme tensions are achieved below 50 mm of depth.

The results from analysis using Huet-Sayegh Model were almost the same to the Burgers Model basing analysis.

In none of the above mentioned constructions at temperature of 40 °C, under either slow or fast movement speed, the risk of permanent, plastic deformations doesn't occur. Innovative constructions "I" behave better then typical construction "T" under slower movement.

The most important aspects of the permanent, viscous deformation were gathered on Figure 10. In every types of the construction familiar strain occurred. The slower movement is, the strain of the construction is higher.

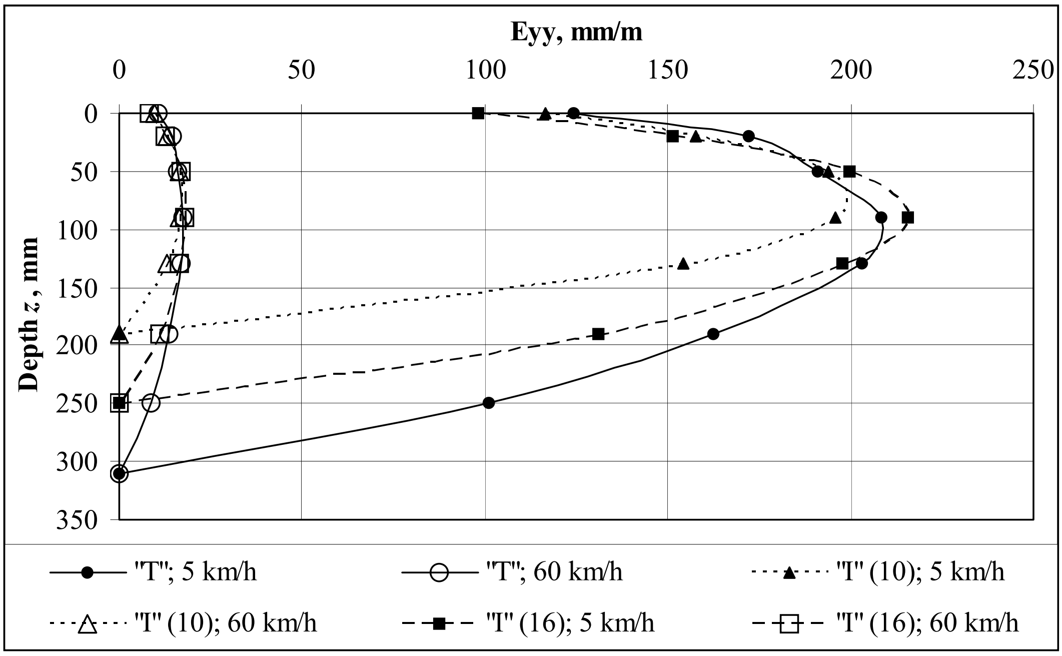

Figure 10: Permanent, viscous horizontal strain

The difference between the asphalt layer thickness in innovative constructions “I” caused the differences in the stress amount. In the innovative construction “I” (10) at thickness smaller of about 15 %, strain is slighter of about 10 % at speed of 5 km/h (for speed of 60 km/h these differences are small enough to omit). Conclusion is that to avoid the permanent deformations, thin asphalt constructions should be applied. Also comparing the typical construction “T” to the innovative construction “I” (16), where the first one is thicker, relationship is opposite. It shows that amount of strain depends not only on the layer thickness but also the properties of applied material.
Figure 10 indicates that extreme strain is achieved at depth of about 50 – 100 mm. In this zone, in every type of construction extreme strain was achieved. This phenomenon has an explanation, for example it is caused by poor resistance of the binder course for permanent deformation. It has no confirm in the 3-axis viscosity test though (Figure 4). In case of typical construction “T” the wearing course is more vulnerable for strain than lower courses. In case of the innovative constructions, the wearing course has greater viscosity (this parameter was taken to the calculations) than lower courses. The above facts show that strain below the top of the construction don’t depend directly on material’s parameters.
Occurrence of the extreme dislocations below the surface of the course gives a sign, that the most rut resistant should be the binder course. This observation is particularly important in the renovation of the pavements. Coverage of an old, low deformation-resistant asphalt course, by new, deformation resistant, it will not certainly prevent the rutting of the repaired pavement, even it may multiply the deformation in an old layer, by placing it in the bigger strain area.

SUMMARY

Mechanistic pavement design is a very complex task. It requires either reliable mechanical parameters or proper model of pavement behaviour. Elastic model is well-known, easy and understandable, but it simplifies real behaviour of bituminous materials. Viscoelastic model used in VEROAD software enable to simulate viscoelastic nature of asphalt layers and moving of loading wheel. VEROAD software was positively validated on LINTRACK simulator.
The set of asphalt mixes were designed and subjected to wide range of laboratory tests. Results were used in analysis of behaviour of typical and innovative flexible pavement structures. The following conclusions can be drawn:

- both structures met requirements for heavy traffic,
- fatigue life of thinner innovative structure is closed to fatigue life of typical structure,
- innovative structure enables to reduce thickness of asphalt layers,
- there is a significant difference between fatigue life of innovative structures calculated with IA fatigue law or fatigue laws from direct laboratory tests - IA method doesn’t show advantages of novel materials,
- calculations based on viscoelastic models lead to higher strain values and safer solution of structure comparing with elastic models,

- VEROAD software enables to find maximum strain at a bottom of asphalt layer, that is not under the centre of wheel as it is taken in elastic model,
- speed of moving wheel is one of critical factors that influence fatigue life as well as permanent deformations and design of asphalt pavement; it should be taken into account, e.g. in design of slow heavy traffic lanes,
- tensile strains appear on the surface of pavement, this confirms the observations of fatigue cracking induced in upper part of pavement structures by overloaded trucks; use of novel materials improving fatigue resistance of wearing courses is then justified,
- three of the constructions indicated permanent, viscous and plastic deformation resistance,
- in thinner asphalt constructions the strain is slightly lower,
- the lowest principal stress are generated on the surface of asphalt layers, where comparably less resistant material could be used (asphalt mixes with bigger amount of soft bitumen for thin layers),
- at higher vehicle speeds the biggest principal stress are generated at the bottom of asphalt courses, where adequately more durable materials should be used (high stiffness modulus mixes),
- the highest deformations of asphalt layers occur in lower layers of the pavement structure (at depth of about 40 – 100 mm), where the most permanent deformation resistant materials should be applied; it should be respected both in pavement design and pavement rehabilitation,
- full scale accelerated tests should be performed for better evaluation of novel materials and pavement construction methods as well as for estimation of shift factors for laboratory fatigue laws and permanent deformation behaviour.

REFERENCES

Sybilski D. et al. (1997), *Katalog Typowych Konstrukcji Nawierzchni Podatnych i Półsztywnych*, Ed. by IBDiM, GDDP, Warsaw, Poland, 1997

Sybilski D. et al. (2002), *Zasady wykonywania nawierzchni asfaltowej o zwiększonej odporności na koleinowanie i zmęczenie (ZW-WMS 2002)*, Seria informacje i instrukcje, zeszyt 63, Ed. by IBDiM, Warsaw, Poland

Standard test method for determining the fatigue life of compacted hot mix asphalt (HMA) subjected to repeated flexural bending, AASHTO TP8-94 (1994)

Cominsky R.J. (1994), *The Superpave Mix Design Manual for New Construction and Overlays*. SHRP-A-407, Washington, USA

French Design Manual for Pavement Structures, SETRA, LCPC (1997)

Hopman P., Nilsson R., Pronk A. (1997), *Theory, validation and application of the disco-elastic multilayer program VEROAD*, ICAP, Seattle, USA

Bituminous mixtures − Test methods for hot mix asphalt − Part 25: Cyclic compression test, part B: Triaxial cyclic compression test, prEN 12697−25

Molenaar J. M. M., Molenaar A. A. A. (2000), *Susceptibility to permanent strain of asphalt in the dynamic triaxial compression creep test*, 2-th Euroasphalt & Eurobitume Congress Barcelona 2000 – Proc.0095.uk

Hopman P., Nilsson R., Isacsson U. (2001), *Influence of different rheological models on predicted pavement responses in flexible pavements*, KTH Report, Stockholm